A study of the bilinear-biquadratic spin-1 antiferromagnetic chain using the valence-bond basis

1989 J. Phys.: Condens. Matter 1 153

(http://iopscience.iop.org/0953-8984/1/1/014)

J. Phys.: Condens. Matter **1** (1989) 153–167. Printed in the UK

A study of the bilinear–biquadratic spin-1 antiferromagnetic chain using the valence-bond basis

Kenneth Chang†, Ian Affleck‡§, Geoffrey W Hayden‖ and Zoltan G Soos‖

† Department of Physics, University of Illinois, Urbana, IL 61801, USA
‡ Canadian Institute for Advanced Research, and Physics Department, University of British Columbia, Vancouver, BC V6T 2A6, Canada
‖ Department of Chemistry, Princeton University, Princeton, NJ 08544, USA

Received 28 June 1988

Abstract. An efficient valence-bond technique is introduced for the numerical study of singlet states of spin-1 antiferromagnetic chains and is applied to the general bilinear–biquadratic Hamiltonian. The results support the hypothesis that the gap first vanishes, with increasing biquadratic exchange, at the Bethe *ansatz* integrable point, which separates regular and dimerised regimes. We distinguish between real gaps and the mixing of degenerate ground states due to quantum tunnelling in small systems.

1. Introduction

Quantum spin chains have been a subject of theoretical fascination, and experimental application, for almost 60 years. A large variety of theoretical techniques have been applied, including exact solutions by the Bethe *ansatz*, exact numerical diagonalisation of finite chains and approximate mappings onto quantum-field theories. Renewed interest in these chains is due to a provocative argument by Haldane [1] that the spin-1 antiferromagnetic Heisenberg model has qualitatively different low-energy behaviour than the spin-$\frac{1}{2}$ model, which was solved by Bethe [2] and has gapless excitations. A number of papers have appeared [3, 4] reporting numerical work on the gap for the spin-1 Heisenberg model. Despite some early dissent, most workers now agree that the gap is indeed non-zero. Experimental evidence for a gap has also been obtained from neutron scattering experiments [5] on $CsNiCl_3$.

Haldane's arguments [1] that the spin-1 chain has a gap appear to be contradicted by the existence of a bilinear–biquadratic antiferromagnetic Hamiltonian

$$H = \sum_i [S_i \cdot S_{i+1} - \beta(S_i \cdot S_{i+1})^2] \tag{1}$$

which is solvable [6] by the Bethe *ansatz* at $\beta = 1$ and *does not* have a gap there. A proper understanding of this issue requires consideration of general β in equation (1). A phase diagram for the model has been proposed [7, 8], using approximate field-theory

§ Research supported in part by the Natural Sciences and Engineering Research Council of Canada.

0953-8984/89/010153 + 15 $02.50

mappings, with a unique ground state and a gap for $\beta < 1$. The value $\beta = 1$ is a critical point where the gap vanishes. For $\beta > 1$ the ground state of the infinite chain is twofold degenerate due to a dimerisation or doubling of the unit cell, and there is also a gap in this region.

The only rigorous support for this phase diagram comes from the exact solution of the $\beta = -\frac{1}{3}$ model, in terms of valence bonds [9], where the ground state is unique and there is a gap. Several papers have also appeared reporting numerical work on the general bilinear–biquadratic Hamiltonian [10, 11]. The gap persists for some range of β near zero, but first vanishes at a value of β somewhat less than 1. Furthermore, they conclude that the gap remains zero for all larger values of β. The focus has been on the gap to the lowest excited state, which is generally a triplet ($S_T = 1$) rather than a singlet. The present work considers only singlet excited states. However, if the triplet gap vanishes, the singlet gap should also vanish, because two separated localised low-energy triplet excitations on the chain can be combined as a low-energy singlet excitation.

Most finite chain diagonalisation has been performed using the standard basis of S_z eigen-states. However, an alternative approach has also been used [12] for studying sectors with fixed total spin S_T. For example, a basis of singlet states, $S_T = 0$, is constructed out of 'valence bonds', or contractions of two spin-$\frac{1}{2}$ variables to form a singlet. A complete set of singlets is obtained by all such pairwise contractions of spins. An arbitrary state of this type, for an $s = \frac{1}{2}$ chain, can be represented by a set of lines connecting the pairs of contracted points, as in figure 1. This basis has lower dimension than the set of $S_{zT} = 0$ states. Also, certain Hamiltonians have exact ground states which can be written simply in terms of valence bonds [9, 13]. Furthermore, valence bonds provide an intuitive way of thinking about the ground state of an antiferromagnet which is quite different from the usual Néel state and in some cases more useful. This approach has been used by Anderson [14] and others to discuss certain properties of the recently discovered high-T_c superconductors.

In this paper, we will develop the valence-bond basis into an efficient tool for performing exact numerical diagonalisations of spin-1 chains. We will then use this basis to study energy gaps in the bilinear–biquadratic Hamiltonian with $\beta \geqslant 0$ for chains of length up to 16. At the special point $\beta = \infty$, the purely biquadratic model, there is a special SU(3) symmetry [7]. The number of SU(3) invariant states at $\beta = \infty$ is the same as the number of SU(2) invariant (i.e. spin singlet) states for an $s = \frac{1}{2}$ Heisenberg chain; indeed the two models are simply related to each other in the singlet sector. Thus longer chains can be studied at $\beta = \infty$ and exact gaps for chains of length up to 26 are discussed.

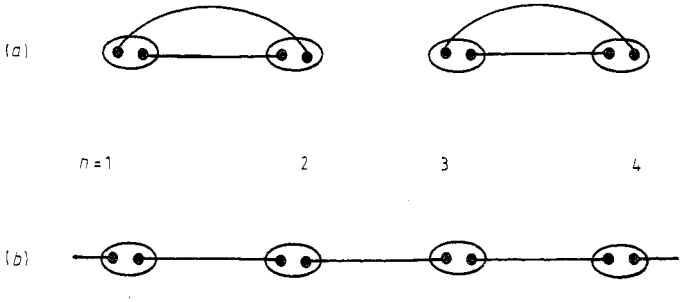

Figure 1. (*a*) The dimerised state for an $s = 1$ chain. $S = 1$ sites are split into pairs of $s = \frac{1}{2}$ sites. Valence bonds singlet couple the $s = \frac{1}{2}$ sites. (*b*) The valence-bond solid state for an $s = 1$ chain.

In the next section we will review some facts about the valence-bond basis for $s = \frac{1}{2}$ sites, develop the necessary techniques for extending it to $s = 1$ sites, and present our calculations. In § 3, we will show how our numerical data support the hypothesised phase diagram for the bilinear–biquadratic model. In § 4 we will review the special SU(3) symmetry of the biquadratic model, and discuss its implications for numerical work. Section 5 is a brief conclusion.

2. The valence-bond basis

In numerical diagonalisation of finite chains, it is important to reduce the size of the Hilbert space, using symmetries, as much as possible. Thus it is standard to work in a subspace of definite total S_{zT}, momentum and parity. However, most previous work has *not* projected out the subspace of definite total S_T^2. This is due to the difficulty of working with states of definite S_T^2.

In the spin-$\frac{1}{2}$ case a convenient basis [15] was found long ago and is known as the valence-bond basis [12]. The most general way to form a singlet out of a collection of N spin-$\frac{1}{2}$ variables is to contract them pairwise to form singlets. (This is essentially the statement that there is only one invariant tensor for SU(2).) We represent such a singlet contraction as

$$\varepsilon^{\alpha\beta}|_{\alpha\beta}\rangle = |-\tfrac{1}{2}, \tfrac{1}{2}\rangle - |\tfrac{1}{2}, -\tfrac{1}{2}\rangle \tag{2}$$

(α, β take on the values $\pm\frac{1}{2}$, and repeated indices are summed.) It is actually more convenient to raise the index on the even sites, defining

$$|^{\alpha}\rangle \equiv \varepsilon^{\alpha\beta}|_{\beta}\rangle. \tag{3}$$

(In fermion language this corresponds to making a particle–hole transformation.) A singlet contraction between an odd and an even site can then be written $|_{\alpha}{}^{\alpha}\rangle$.

We may represent an arbitrary singlet diagrammatically by drawing lines between the pairs of contracted spins. An important reduction occurs because we may leave out any diagram with crossed lines. This follows [12] from the 'uncrossing identity'

$$\varepsilon^{\alpha\beta}\varepsilon^{\gamma\delta} = \varepsilon^{\alpha\gamma}\varepsilon^{\beta\delta} - \varepsilon^{\alpha\delta}\varepsilon^{\beta\gamma}. \tag{4}$$

The uncrossed diagrams can, in fact, be shown to be linearly independent [16] by simply counting the number of states for a chain of length L. The number N_0 of $S_T = 0$ states is the number of $S_{zT} = 0$ states minus the number of $S_{zT} = 1$ states, since all spin multiplets of higher S_T have an $S_{zT} = 1$ element, as well as an $S_{zT} = 0$ element, whereas the $S_T = 0$ states do not. Thus [12]

$$N_0 = L!/(L/2)!(L/2)! - L!/(L/2+1)!(L/2-1)! = L!/(L/2)!(L/2+1)!. \tag{5}$$

We now count the number of uncrossed valence-bond states. Each such state is equivalent to a random walk on the positive real axis which begins and ends at the origin. Successive points on the chain correspond to successive steps, with the step direction being the direction that the valence bond goes from that point, and the step length being one. The valence bond from the first point necessarily goes to the right and after n steps the total number of valence bonds which have gone to the right must be at least as big as the number that have gone to the left. Hence the random walk is restricted to the positive axis. The *total* number of random walks beginning and ending at the origin is $L!/(L/2)!(L/2)!$. The number of random walks beginning and ending at the origin which

go negative somewhere equals the *total* number beginning at the origin and ending at -2. This follows from taking any random walk which goes negative and begins and ends at the origin and reflecting the section of the walk from the last (-1) about the point (-1). This number is $L!/(L/2+1)!(L/2-1)!$. The difference of these numbers, the total number of uncrossed valence-bond configurations, is the same as the number of singlets, proving the linear independence of this basis.

By working in the subspace with $S_T = 0$, instead of the subspace with $S_{zT} = 0$, we reduce the number of states by a factor of $1/(L+1)$. This means that the chain length can be increased, for example from 22 to 26 by working in the $S_T = 0$ subspace without significantly increasing the number of states. There are 705 432 $S_{zT} = 0$ states for a chain of 22 sites and 742 900 $S_T = 0$ states for a chain of 26 sites. These numbers can be reduced by about another factor of 50 by projecting out states of definite momentum and parity.

There is one rather unusual feature of the valence-bond basis: it is not orthonormal. The simplest way to proceed [12] is *not* to calculate matrix elements of the Hamiltonian H in this basis $\langle\psi_i|H|\psi_j\rangle$, but rather to define a non-symmetric matrix h_{ij} by expressing the action of H on any state as a linear combination of the states

$$H|\psi_i\rangle = \sum_j h_{ij}|\psi_j\rangle. \tag{6}$$

The matrix h is unique due to the linear independence of the states. The eigenvalues and left eigenvectors of h give those of H. The matrix h has the important advantage of being sparse. To see this, we consider [17] the bilinear Hamiltonian for $s = \frac{1}{2}$:

$$H = \sum_i [S_i \cdot S_{1+1} - \tfrac{1}{4}] \equiv \sum_i (-\theta_{i,i+1}/2). \tag{7}$$

Thus, a valence bond across sites $i, i+1$ is an eigenstate of $-\theta_{i,i+1}$ with eigenvalue 2. More general cases can be worked out by using the fermionic representation of the spin operators

$$S = \tfrac{1}{2}\psi^{+\alpha}\sigma_\alpha{}^\beta\psi_\beta \tag{8}$$

or simply by checking each term. For a chain of four sites, let us consider the action of the term in H acting between the second and third site, on a state with valence bonds between the first two and last two sites:

$$H_{23}|_\alpha{}^\alpha{}_\beta{}^\beta\rangle = -\tfrac{1}{2}|_\alpha{}^\beta{}_\beta{}^\alpha\rangle. \tag{9}$$

The two bonds terminating at the end-points of the link are broken, a bond is formed on the link, and the two remaining dangling bonds are contracted. This actually expresses the action of H on an arbitrary link not containing a valence bond [17]. Note that we obtain a single valence-bond state, thereby preserving the sparseness of the usual basis. It then follows that the number of non-zero off-diagonal entries in any row of h is less than L. Of course, for configurations with many nearest-neighbour valence bonds in them the number of diagonal terms obtained is close to $L/2$.

This valence-bond basis [12] has been used extensively for calculations involving $s = \frac{1}{2}$ chains and Hubbard or other quantum cell models. In this paper we will generalise it to the case of $s = 1$. Again it allows a significant increase in the chain length possible for a given amount of computer time and storage. We note that a spin-1 variable can be obtained by symmetrising two spin-$\frac{1}{2}$'s. Thus we will put two spin-$\frac{1}{2}$ variables on each site, consider arbitrary singlet states, and at the end, symmetrise with respect to the pair of spins on each site. This symmetrisation will set to zero any diagram with the two spins

on a single site contracted. Examples of valence-bond diagrams connecting spin-1 sites are given in figure 1.

The spin-1 bilinear–biquadratic Hamiltonian can be written in terms of the spin-$\frac{1}{2}$ variables. Labelling two neighbouring $s = 1$ spins, S_1, S_{11} with $S_1 \equiv S_1 + S_2$, $S_{11} \equiv S_3 + S_4$, the spin-1 Heisenberg interaction in equation (1) contains coupling between first, second and third spin-$\frac{1}{2}$ neighbours. Non-nearest-neighbour coupling produces linearly dependent crossed diagrams. Fortunately, these interactions can be rewritten [12] in terms of products of nearest-neighbour ones using

$$S_i \cdot S_j = 2(S_i \cdot S_k)(S_j \cdot S_k) + 2(S_j \cdot S_k)(S_i \cdot S_k) \tag{10}$$

which follows from the spin-$\frac{1}{2}$ anticommutator

$$S^a S^b + S^b S^a = \tfrac{1}{2}\delta^{ab}. \tag{11}$$

For i and j equal to 1 and 3:

$$S_1 \cdot S_3 = \tfrac{1}{2}(\theta_{12}\theta_{23} + \theta_{23}\theta_{12} - \theta_{12} - \theta_{23}) + \tfrac{1}{4} \tag{12}$$

in terms of the θ_{ij} operators defined in equation (7). Note that the first term $\theta_{12}\theta_{23}$ produces states with a valence bond between the first and second spin-$\frac{1}{2}$'s which are both on the same site. This corresponds to spin-0 on the site instead of spin-1 as required. In writing H in terms of these fictitious $s = \frac{1}{2}$ spins, we may project out the $s = 1$ part of the final state for each site, or simply eliminate all diagrams with a valence bond between two $s = \frac{1}{2}$ spins on the same site, i.e. 12 or 34. We can also rewrite $S_1 \cdot S_4$ in terms of nearest-neighbour interactions by using equation (10) twice. Dropping the terms which produce on-site valence bonds, we finally obtain

$$S_1 \cdot S_{11} = -\tfrac{1}{2}\theta_{23}\theta_{12}\theta_{34} + \theta_{23}\theta_{12} + \theta_{23}\theta_{34} - 2\theta_{23} + 1. \tag{13}$$

In a similar manner, squaring this term, the biquadratic interaction leads after some algebra to nearest-neighbour products of θ_{ij} operators [18].

The spin-1 problem is thus reduced to a spin-$\frac{1}{2}$ problem with twice as many spins, and certain diagrams set to zero. It can be checked that the set of diagrams that we are keeping form a linearly independent basis. This follows from the linear independence of the $s = \frac{1}{2}$ basis. The number of states with $S_{zT} = 0$ for a spin-1 chain of length L (even) is

$$\sum_{m=0}^{L/2} L!/(m!)^2(L-2m)! \tag{14}$$

for m sites with spin $S_z = 1$ or -1, and the remaining $L - 2m$ sites with $S_z = 0$. The number of states with $S_T = 0$ can again be obtained by subtracting from this number the number of states with $S_{zT} = 1$, giving [18]

$$N_0 = \sum_{m=0}^{L/2} L!/(m!)^2(L-2m)! - \sum_{m=0}^{L/2-1} L!/(m!)(m+1)!(L-2m-1)!. \tag{15}$$

For a spin-1 chain of length 16 the number of $S_{zT} = 0$ and $S_T = 0$ states is respectively 5196627 and 227475, a reduction by about a factor of 23. Working in the subspace of definite momentum and parity reduces this number to about 8000.

We have calculated the excitation energy of the first excited state $E_{\pi+}$ (momentum π, parity even), second excited state $E_{\pi-}$ (momentum π, parity odd) and E_{0-} (momentum 0, parity odd) for β between 0 and ∞ for chains of length up to $L = 14$, and for a few values

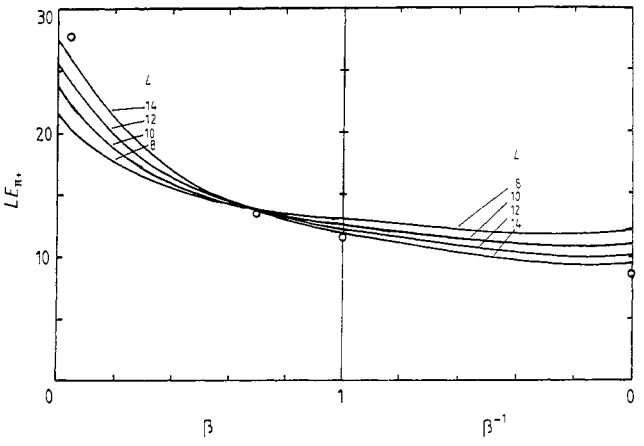

Figure 2. The scaled excitation energy of the lowest momentum π, parity-even state, LE_{π_+} versus β. Data for $L = 16$ are indicated by open circles.

of β, $L = 16$, where each eigenvalue takes about 10 h to compute on a VAX 11/780. The ground-state energy at $\beta = 0$ agrees with Nightingale and Blote's result [4]. Additional checks were obtained at $\beta = \infty$ by comparison with independent valence-bond (VB) calculations for modified spin-$\frac{1}{2}$ Heisenberg rings, as a consequence of the mapping described in § 4. The $\beta = 0$ and ∞ tests give separate checks for the quadratic and biquadratic terms in equation (1). Convergence to 10^{-7} was sought. The definition of the Hamiltonian in equation (1) involves an arbitrary β-dependent multiplicative factor. Note that for a chain of two sites the gap between the ground state (of total spin 0) and the highest energy state (of total spin 2) is $3(1 + \beta)$. Thus we choose to normalise our Hamiltonian, equation (1), by a factor of $(1 + \beta)$ in order to avoid β-dependent structure in the energies. The scaled gaps LE_{π_+}, LE_{0_-} and LE_{π_-} are plotted against β for $0 < \beta < 1$ on the left side and against $1/\beta$ for $1 < \beta < \infty$ on the right side of figures 2, 3 and 4 respectively. Data were obtained at intervals of 0.05 in β and $1/\beta$.

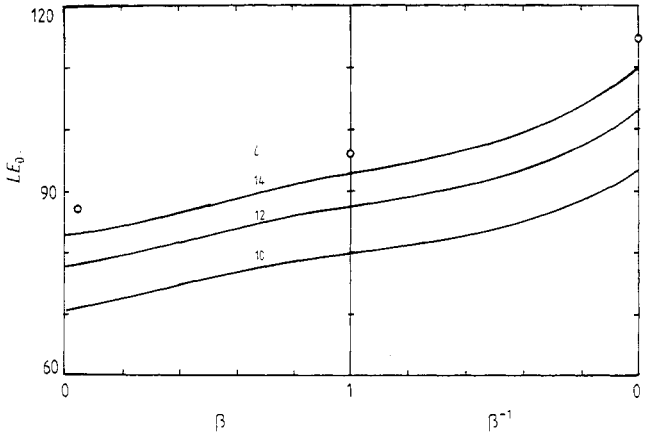

Figure 3. The scaled excitation energy of the lowest momentum 0, parity-odd state, LE_{0_-} versus β. Data for $L = 16$ are indicated by open circles.

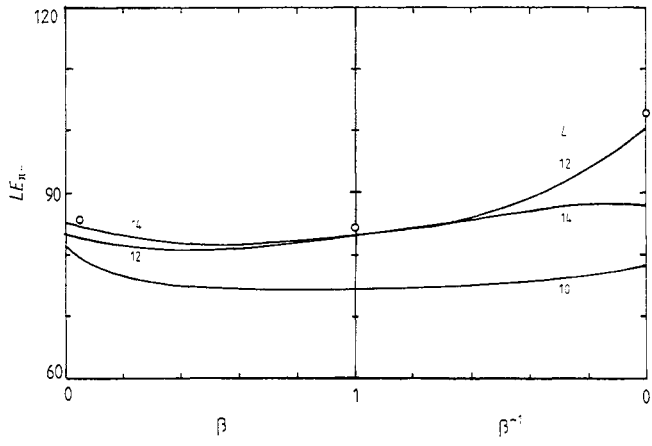

Figure 4. The scaled excitation energy of the lowest momentum π, parity-odd state, LE_{π^-} versus β. Data for $L = 16$ are indicated by open circles.

3. Hypothesised phase diagram of the bilinear–biquadratic Hamiltonian

The spin-1 Heisenberg (i.e. bilinear) Hamiltonian was predicted to have a gap by Haldane [1]. However, the Bethe *ansatz* [6] shows the bilinear–biquadratic Hamiltonian with $\beta = 1$ to have no gap. A phase diagram has been proposed [7, 8] for the general bilinear–biquadratic case which is consistent with these two results. In general, gapless spin chains are expected to have a low-energy sector which is equivalent to a massless quantum-field theory. The spin-wave velocity and $T \to 0$ susceptibility and specific heat, calculated exactly from the Bethe *ansatz* [6], agree exactly with predictions [7, 8, 19] of a particular massless quantum-field theory, known as the Wess–Zumino–Witten non-linear σ model (WZW model) with topological coupling constant $k = 2$. Also, recent calculations of the finite-size energy gaps agree well with this theory [20]. There is a relevant operator which can be added to the WZW Hamiltonian. It is expected to produce a gap, and for one sign of the coupling constant but not the other lead to a breaking of the symmetry of translation by one site, dimerisation. Thus, moving away from $\beta = 1$ should generate this operator and produce a gap. For $\beta < 1$, the ground state is unique, but for $\beta > 1$ it is twofold degenerate owing to the spontaneous breaking of the translational symmetry by dimerisation.

The valence-bond basis provides simple variational ground states for the two different phases. The broken symmetry phase can be represented by the dimerised state with two valence bonds connecting pairs of neighbouring sites, as in figure 1(*a*). There are two such states related by translation by one site. The phase of unbroken symmetry can be represented by the valence-bond solid state with a single valence bond connecting each pair of neighbouring sites as in figure 1(*b*). This in fact turns out to be the exact ground state for $\beta = -\frac{1}{3}$, where there is indeed a gap [9]. These two states are variational ground states [9] for arbitrary β; the valence-bond solid state has lower energy for $\beta < \frac{1}{2}$ and the dimerised state has lower energy for $\beta > \frac{1}{2}$. The true ground state for arbitrary β is considerably more complicated than these simple states, but is expected to share the symmetry properties of the valence-bond solid state for $\beta < 1$ and of the dimerised state for $\beta > 1$. The value $\beta = 1$ is a critical point separating the two phases where the gap

vanishes. This is somewhat analogous to the critical temperature in the Ising model where the correlation length diverges.

In testing these hypotheses on finite chains, a subtlety emerges, connected with the broken symmetry in the dimerised phase. If we consider some value of $\beta > 1$ where there are two ground states for an infinite chain, then we may think of the two simple dimerised states as being rather like the two minima of a symmetric double-well potential. These configurations are not the exact ground states. Instead, there are some quantum fluctuations away from these states, just as occurs for the quantum-mechanical double-well problem. In fact, if the barrier between the two wells is finite, quantum tunnelling will always mix the two states localised near the bottom of each well. The true ground state is essentially a symmetric linear combination of the two localised states, while the antisymmetric combination has a very low excitation energy. The splitting is entirely due to the quantum tunnelling and is $O[\exp(-S/\hbar)]$, where S is the classical action. In the spin chain problem there is also tunnelling between the two dimerised configurations, but this is suppressed as the chain gets longer. It takes L applications of H to turn one dimerised state into the other. Thus the matrix element between these two states is $O(\varepsilon^L)$ or $O(e^{-aL})$, where ε is some number less than 1 and a is a positive constant. Just as for the double well with a large barrier, the complete low-energy spectrum consists of closely spaced pairs of states with large gaps separating each pair. So the spectrum of a large chain should consist of pairs of states with a gap of $O(1)$ between each pair, but a splitting of $O(e^{-aL})$ separating the two members of each pair. In the infinite chain limit, the splitting vanishes, and the Hilbert space separates into two sectors, corresponding to the two different dimerised ground states.

Thus numerical investigations of the conjecture must carefully distinguish the gap to the partner of the ground state, of $O(e^{-aL})$, and the gaps to the higher pairs of states, of $O(1)$. A small gap to the partner of the ground state is an indication of dimerisation, not of a vanishing gap in the infinite system. The ground state and its partner should have the symmetry of the (respectively) symmetric and antisymmetric linear combinations of the two simple dimerised states. Owing to our sign convention in defining valence bonds, translating one of the simple dimerised states by one site gives the other simple dimerised state times a factor $(-1)^{L/2}$. Thus the ground state, the sum of the two dimerised states, transforms into $(-1)^{L/2}$ times itself under translation by one site; it has momentum $(L/2)\pi$. The partner of the ground state, the difference of the two simple valence-bond states, transforms into $-(-1)^{L/2}$ and so has momentum $(L/2 + 1)\pi$, or π relative to the ground state. Parity, or reflection about the midpoint between two sites, maps either dimerised state into itself, times the same factor $(-1)^{L/2}$. Thus both linear combinations have the same parity, $(-1)^{L/2}$. All momenta and parity in figures 2, 3 and 4 are relative to that of the ground state. We interpret the lowest energy excitation, $E_{\pi+}$ in figure 2, as the antisymmetric combination of ground states, for $\beta > 1$.

One way of testing numerically for dimerisation is to study a chain of odd length. The simple dimerised state now has one unpaired spin, and hence total spin $S_T = 1$. Thus a $S_T = 1$ ground state for a chain of odd length is an indication of dimerisation. It is interesting to note that previous numerical work [10] found a crossover from $S_T = 0$ to $S_T = 1$ with increasing β. While this indicates dimerisation, it does not shed light directly on the gap issue. However, experience with other situations, as for example $s = \frac{1}{2}$ chains, suggests that dimerisation is normally accompanied by a gap, so that evidence for dimerisation may be considered indirect evidence for a gap.

Here we study even chains. In § 2 we presented numerical results for the scaled gaps, $LE_{\pi+}$, LE_{0-} and $LE_{\pi-}$. Perhaps the most dramatic feature is the crossing of the smallest

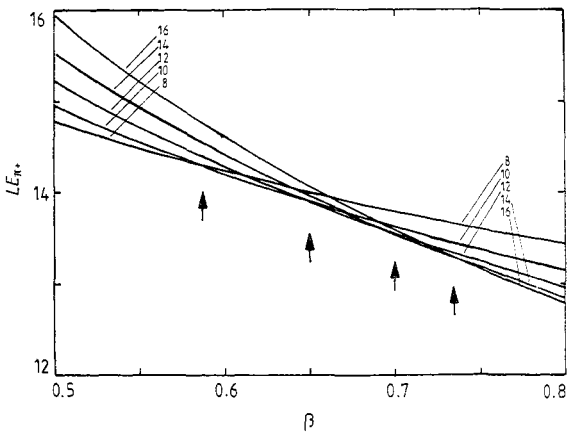

Figure 5. A blow-up of figure 2, showing the crossings of the curves for different values of L.

scaled gap, $LE_{\pi+}$, for different values of β as shown in figure 5 by expanding the $0.5 < \beta < 0.8$ region of figure 2. According to field-theory arguments the scaled gap diverges as L in the region with a gap, but becomes exponentially small in the dimerised phase. It follows that $LE_{\pi+}$ must cross at least once with increasing β and at large L must approach a constant near $\beta = 1$, separating the two phases. For sufficiently small β the scaled gap increases with L, but for larger β it decreases, thus producing crossing points in figure 5 for $L, L + 2$ pairs that should converge to $\beta = 1$ as $L \rightarrow \infty$. Since this asymptotic scaling behaviour should set in once L is longer than the (β-dependent) correlation length, crossings should occur even for only moderately large L. The crossing points of the L and $L + 2$ curves are plotted versus $1/(L + 1)$ in figure 6. The crossing points are

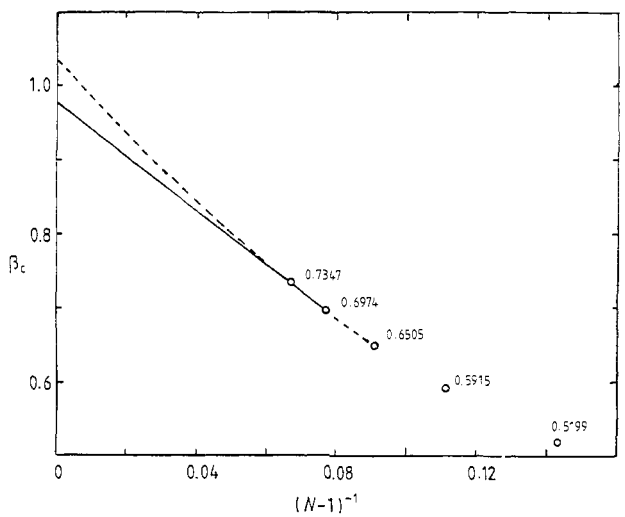

Figure 6. The crossing points of the L and $L + 2$ curves of $LE_{\pi+}$ versus β, plotted against $1/(L + 1)$. Linear and quadratic extrapolations are indicated by the full and broken curves, respectively.

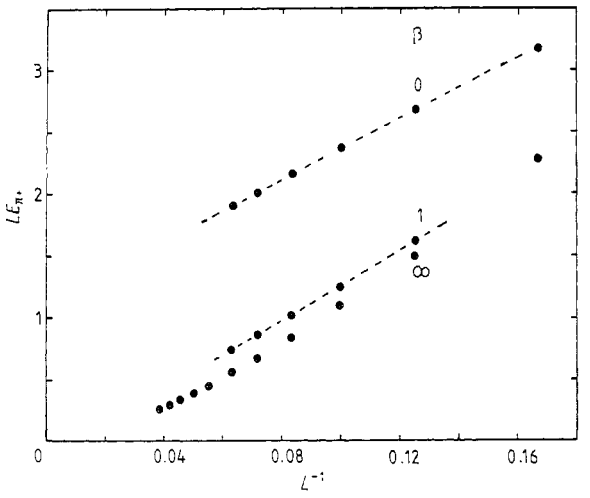

Figure 7. $E_{\pi+}$ versus $1/L$ for $\beta = 0$, 1 and ∞.

seen to increase monotonically with a decreasing curvature. Assuming that this trend continues with positive curvature, a lower bound on β_c is found from a straight-line extrapolation of any two points. An upper bound is given by fitting a parabola to three successive points. The $N \leqslant 16$ data in figure 6 lead to $\beta_c = 1.01 \pm 0.03$. Similar extrapolations [10, 11] for the triplet gap suggested a smaller critical value of β around 0.6. We note that for the singlet gap the critical value of β is clearly much higher, the crossing already occurring at 0.73 for the $L = 14$, $L = 16$ curves. This technique for estimating β_c is better motivated for the singlet, momentum π-scaled gap where the theory predicts that crossing *must* occur at β_c.

The scaled gaps $LE_{\pi+}(L)$ of figure 2 have no crossings for $\beta > 1$ and decrease with increasing L in this region. The gap $E_{\pi+}$ is plotted against $1/L$ in figure 7 for $\beta = 0$, 1 and ∞. At $\beta = \infty$ data up to $L = 26$ are included using the mapping discussed in § 4, while at other values the maximum is $L = 16$. Once again, a finite gap is suggested at $\beta = 0$ along with vanishing gaps at $\beta = 1$ and ∞. The $\beta = 0$ singlet gap extrapolates to roughly 1.0, while the $\beta = 0$ triplet gap [4] is about 0.40 (in units of the spin coupling J). The vanishing $E_{\pi+}$ for $\beta > 1$ is interpreted as dimerisation.

We now turn to the higher excitation energies E_{0-} and $E_{\pi-}$. We expect these to be finite at $L \to \infty$ for all β except $\beta = 1$. As shown in figure 3 E_{0-} is a slowly decreasing function of L. There is no particular structure near $\beta = 1$ and no crossing of the scaled gaps. The scaled excitation energy $LE_{\pi-}$ in figure 4 has similar behaviour except that successive lengths $L = 4n - 2$, $4n$ cross at large β. The families of curves with $L = 4n$ and $L = 4n - 2$ seem quite different at large β. Possibly this is some indication of dimerisation at large β but we do not have even a qualitative explanation of it. Plots of E_{0-} (figure 8) and $E_{\pi-}$ versus $1/L$ at $\beta = 0$, 1 and ∞ for L up to 16 lead to no definitive conclusion concerning the gap for $L = \infty$. In particular, $E_{0-}(0)$ extrapolates nicely to roughly 3.0, or to about $3E_{\pi+}(0)$. The $L \leqslant 16$ values of $E_{0-}(1)$ and $E_{0-}(\infty)$ exceed $E_{0-}(0)$, but their slope in figure 8 is greater and less linear. The field-theory prediction, that $E_{0-}(1) \to 0$ as $L \to \infty$ while $E_{0-}(\infty)$ remains finite, cannot be tested without going to considerably larger L.

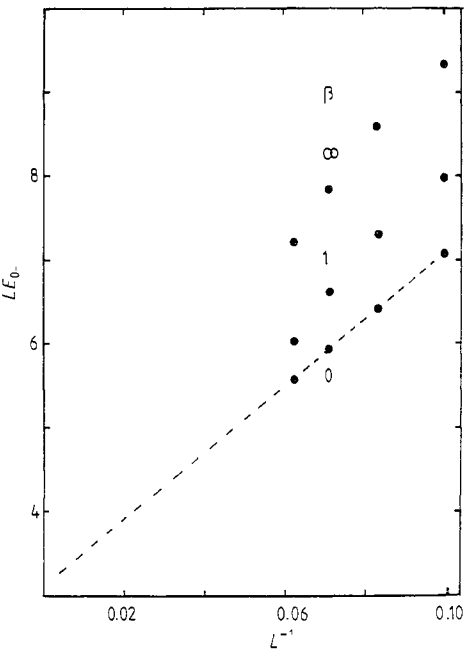

Figure 8. E_{0-} versus $1/L$ for $\beta = 0$, 1 and ∞. Linear extrapolation is indicated for $\beta = 0$.

All scaled excitation energies LE_i except $LE_{\pi+}$ should be linear in L for $\beta > 1$ and $\beta < 1$, being constant only at $\beta = 1$. There is no general reason why these curves should necessarily cross, although they could. Field-theory arguments at $\beta = 1$, checked in some cases against Bethe *ansatz* results, suggest that various scaled excitation energies converge as

$$LE_i(L) \to \text{constant} + c_i/\ln L \tag{16}$$

where the c_i are constants [20]. If the c_i are negative then no crossings need occur, as illustrated in figure 9(*a*), while positive c_i lead to at least two crossings as shown in figure 9(*b*). In fact, for singlet states the c_i are positive. However, the above asymptotic scaling at $\beta = 1$ has corrections which are only suppressed by additional powers of $\ln L$, so LE_i may not become a decreasing function at $\beta = 1$, and hence crossings may not occur, until L is very (i.e. exponentially) large. On the other hand, for the lowest triplet state, studied in [20], c_i is negative so LE_i is increasing at large L and no crossings need occur. Explicit Bethe *ansatz* calculations show [20] that the triplet excitation energy, LE_t *does* increase at large L (>20). However for the smaller values of L ($\leqslant$12) used in [10, 11], LE_t is actually decreasing and crossings occur. As L increases, it is likely that the crossings will eventually disappear, rather than converging to $\beta = 1$.

4. SU(3) symmetry of the pure biquadratic model

The pure biquadratic spin-1 model (formally, $\beta \to \infty$) has an SU(3) symmetry [7]. To see this it is convenient to adopt a basis of states on each site which is different from the standard S_z eigen-states or the double spin-$\frac{1}{2}$ states $|_{\alpha\beta}\rangle$. The three states are labelled by

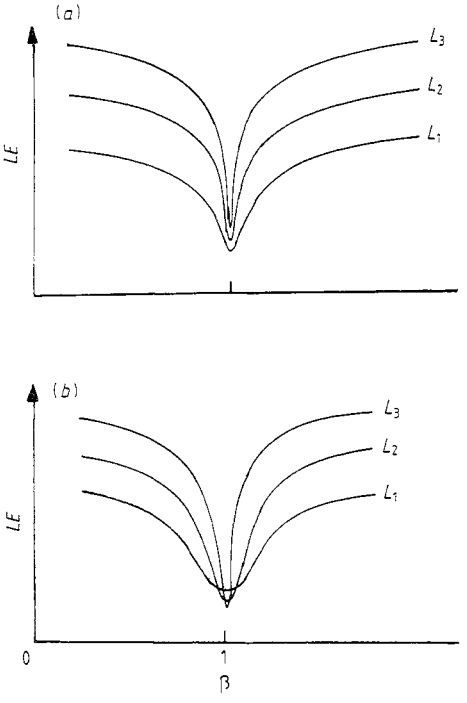

Figure 9. (*a*) Qualitative sketch of scaled excitation energies versus β for c_i negative. (*b*) Qualitative sketch of scaled excitation energies versus β for c_i positive.

an index a which runs from 1 to 3, and are transformed by the spin-1 operators as

$$S^a|b\rangle = i\varepsilon^{abc}|c\rangle \tag{17}$$

where ε^{abc} is the antisymmetric three-index tensor, with $\varepsilon^{123} = 1$. Repeated indices are summed from 1 to 3. Note that $|a\rangle$ is the zero eigenstate of S^a. This basis corresponds to the zero-field states of triplets [21]. No significance is attached to raised or lowered indices for SO(3) representatations. The action of the Heisenberg Hamiltonian on this basis is given by

$$\boldsymbol{S}_i \cdot \boldsymbol{S}_{i+1}|ab\rangle = |ba\rangle - \delta^{ab}|cc\rangle. \tag{18}$$

By applying this tranformation twice we see that the action of the biquadratic term is

$$[(\boldsymbol{S}_i \cdot \boldsymbol{S}_{i+1})^2 - 1]|ab\rangle = \delta^{ab}|cc\rangle. \tag{19}$$

For arbitrary β the bilinear–biquadratic Hamiltonian is invariant under SO(3) rotations:

$$|a\rangle \rightarrow R^{ab}|b\rangle \tag{20}$$

where R^{ab} is an SO(3) rotation matrix, R^{ab} is real, $R^{-1} = R^{\mathrm{T}}$ and $\det R = 1$. However, the pure biquadratic Hamiltonian is invariant under a larger symmetry group of SU(3) transformations. These are defined by an SU(3) matrix $U_a{}^b$ which is a *complex* matrix obeying $U^{-1} = U^{+}$, $\det U = 1$. U acts differently on even and odd sites. Consequently, we change our notation slightly, lowering the index $|_a\rangle$ on odd sites and raising it $|^a\rangle$ on even sites. Also, the complex conjugate matrix is written with the opposite index

elevation: $U^{*a}{}_b$. Under SU(3) transformations the two types of sites transform as

$$|_a\rangle \to U_a{}^b|_b\rangle \qquad |^a\rangle \to U^{*a}{}_b|^b\rangle. \tag{21}$$

This means that the odd and even sites transform under the fundamental and anti-fundamental representations of SU(3) respectively. The Heisenberg Hamiltonian ($\beta = 0$) is not SU(3)-invariant because the first term in equation (18) is a permutation which switches the two inequivalent types of sites. However the pure biquadratic Hamiltonian *is* SU(3)-invariant since

$$U_a{}^b U^{*c}{}_d \delta_b{}^d = U_a{}^b (U^+)_b{}^c = \delta_a{}^c. \tag{22}$$

The biquadratic $s = 1$ model is closely related to the $s = \frac{1}{2}$ Heisenberg model, so that the SU(3) singlet basis can also be represented by valence bonds. An SU(3) valence bond is equivalent to a double valence bond of the split fermion notation (figure 1(*a*)). For a chain of two sites, the only SU(3) invariant is $|_a{}^a\rangle$. In general for a chain of L sites (L even) the most general singlet is obtained by contracting the index on each odd site with the index on some even site. We can again represent this state by a diagram with lines connecting the contracted sites just as we did for the $s = \frac{1}{2}$ Heisenberg model. The condition that only even–odd contractions occur is in fact equivalent to the no-crossing condition, since any line connecting two even or two odd sites would pass over an odd number of other sites and therefore would cross at least one other line. Thus there is the same number of SU(3) singlet states for the biquadratic $s = 1$ model as for the $s = \frac{1}{2}$ Heisenberg model.

We find it convenient to normalise the biquadratic Hamiltonian

$$H_b = -\tfrac{1}{3}\sum [(S_i \cdot S_{i+1})^2 - 1]. \tag{23}$$

The general effect of H on an arbitrary valence-bond state is summarised by

$$\begin{aligned} H_b|_a{}^a\rangle &= -|_a{}^a\rangle \\ H_{bi,i+1}|_a{}^a{}_b{}^b\rangle &= -(1/n)|_a{}^b{}_b{}^a\rangle \end{aligned} \tag{24}$$

where $n = 3$, and in the second equation $H_{bi,i+1}$ acts on spin-1 sites not connected by valence bonds. The $s = \frac{1}{2}$ Heisenberg Hamiltonian of equation (9) acts in the same way on valence-bond states, except that now $n = 2$. Comparing the two cases we see that there is a smaller tendency for nearest-neighbour valence bonds to rearrange themselves for $n = 3$.

In general, an SU(n)-invariant Hamiltonian can be defined [22], acting on states $|_a\rangle$ and $|^a\rangle$, with a running from 1 to n, by

$$H|_a{}^b\rangle = -(1/n)\delta_a{}^b|_c{}^c\rangle. \tag{25}$$

The action of H on valence-bond states is given by equation (24) with n an arbitrary integer. In fact, we may generalise H on the SU(n) singlet sector by letting n be an arbitrary positive real number. We see that for large n the dimerised state becomes essentially the exact ground state, because the valence-bond-breaking effects become $O(1/n)$. The $n = 3$ case (the biquadratic $s = 1$ model) has a greater tendency to dimerise than the $n = 2$ case ($s = \frac{1}{2}$ bilinear model). Whether or not it actually *does* dimerise is a question which we investigate numerically. The scaled $LE_{\pi+}$ gap is shown in figure 10 for $L \leqslant 26$ as a function of $1/n$.

For ordinary spin chains the ground state is expected to be an SU(2) singlet. This has been proven rigorously in certain cases. Thus it is natural to expect that, when the

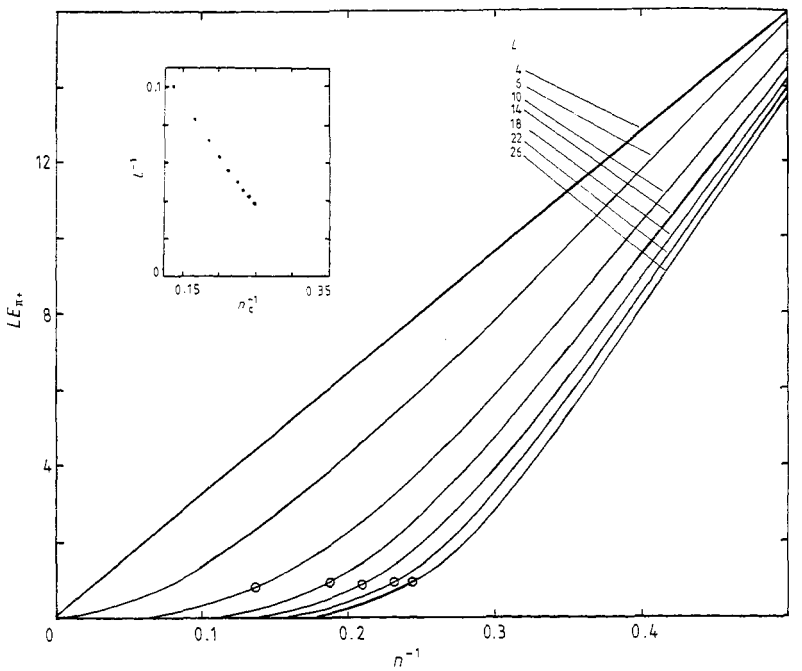

Figure 10. Scaled excitation energies $LE_{\pi+}$ versus $1/n$ for the general SU(n) model. Circles indicate points of maximum curvature. Inset shows $1/L$ versus $1/n_c$ for the point of maximum curvature.

symmetry is SU(3), the ground state will be an SU(3) singlet. However, we do not have a rigorous proof of this. Our numerical diagonalisation of biquadratic chains of length up to 16 in the subspace of SU(2) singlets shows that the ground state is indeed an SU(3) singlet, i.e. it is constructed entirely from double valence bonds, as in figure 1(*a*). We will assume that it is the case for chains of arbitrary length. We report calculations here for biquadratic chains of length up to 26. We also calculate gaps to excited SU(3) singlet states. Using our full solution in the SU(2) singlet subspace for $L \leqslant 16$, we find that the lowest excited state, of momentum π, parity even relative to the ground state, is an SU(3) singlet. As shown in figure 7, $E_{\pi+}(\infty)$ vanishes as $L \to \infty$.

In figure 10 we plot the scaled gap $LE_{\pi+}$ versus $1/n$ for the general SU(n) models, for L up to 26. Numerical results were obtained at intervals of 0.05, except near the points of maximum curvature, indicated by open circles, where the interval is refined to 0.005. This quantity clearly goes to zero rapidly with L for sufficiently large n, and in figure 10 is already indistinguishable from zero by $n = 6$. For $N = 2$ it appears to be converging to a finite constant, consistent with the $1/L$ behavior of the gap in the $s = \frac{1}{2}$ case. This suggests a transition from a dimerised to undimerised, gapless phase with decreasing n. At $L = \infty$, $LE_{\pi+}$ should have a discontinuous derivative at n_c. The inset in figure 10 shows the point $1/n_c$ of maximum curvature as a function of $1/L$, and it appears to be heading towards $n_c \simeq 3$ at $L = \infty$. At this point the curvature is infinite, with a gap opening for $n > n_c$. This is the final evidence for dimerisation of the $\beta \to \infty$, spin-1 chain.

To study the true gap, as explained above we must look at higher excited states. The next two SU(2) singlet excited states are not SU(3) singlets. Nonetheless, we also calculate the excitation energy of the second excited SU(3) singlet state. Extending the

argument given earlier, if there are localised gapless excitations transforming under *any* representation of SU(3) we expect to be able to form an SU(3) singlet excitation by superimposing two distant excitations. Thus the measurement of an SU(3) singlet gap indicates a gap in general. SU(3) gaps were not linear against $1/L$, but curved downward like the $\beta = \infty$ results in figure 8 and made extrapolations inconclusive.

5. Conclusions

The fact that the LE_{π^+} crossing points in figure 6 extrapolate to approximately $\beta = 1$ supports a transition to a gapless state, which is accompanied by dimerisation. The transition is also supported by the plot of LE_{π^+} versus $1/L$ in figure 7, in which there appears to be a gap for $\beta = 0$ but not for $\beta = 1$ or ∞ at $L = \infty$, and by the LE_{π^+} versus $1/n$ plots in figure 10. The excited-state data are more ambiguous, and though a gap is suggested by figures 3 and 4, plots of E versus $1/L$ are inconclusive.

References

[1] Haldane F D M 1983 *Phys. Lett.* **93A** 464; 1983 *Phys. Rev. Lett.* **50** 1153; 1985 *J. Appl. Phys.* **57** 3359
[2] Bethe H 1931 *Z. Phys.* **71** 205
[3] Botet R and Jullien R 1983 *Phys. Rev.* B **27** 613
Botet R, Jullien R and Kolb M 1983 *Phys. Rev.* B **28** 3914
Kolb M, Botet R and Jullien R 1983 *J. Phys. A: Math. Gen.* **16** L673
Parkinson J B, Bonner J C, Muller G, Nightingale M P and Blote H W J 1985 *J. Appl. Phys.* **57** 3319
Schulz H J and Ziman T A L 1986 *Phys. Rev.* B **33** 6545
[4] Nightingale M P and Blote H W J 1986 *Phys. Rev.* B **33** 659
[5] Buyers W, Morra W, Armstrong R, Hogan M, Gerlack P and Hirakawa K 1986 *Phys. Rev. Lett.* **56** 371
[6] Kulish P and Sklyanin E 1982 *Springer Lectures Notes in Physics* vol. 151 (Berlin: Springer) p 61
Kulish P, Reshetikhin N Yu and Sklyanin E 1981 *Lett. Math. Phys.* **5** 393
Takhtajan L 1982 *Phys. Lett.* **87A** 479
Babudjian J 1982 *Phys. Lett.* **90A** 479; 1983 *Nucl. Phys.* B **215** 317
[7] Affleck I 1986 *Nucl. Phys.* B **265** [FS15] 409
[8] Affleck I and Haldane F D M 1987 *Phys. Rev.* B **36** 5291
[9] Affleck I, Kennedy T, Lieb E and Tasaki H 1987 *Phys. Rev. Lett.* **59** 799; 1988 *Commun. Math. Phys.* **115** 477
[10] Solyom J 1987 *Phys. Rev.* B **36** 8642
[11] Oitmaa J, Parkinson J B and Bonner J C 1986 *J. Phys. C: Solid State Phys.* **19** L595
[12] Soos Z G and Ramasesha S *Valence Bond Theory and Chemical Structure* ed. D J Klein and N Trinajstic (Amsterdam: Elsevier) at press
Ramasesha S and Soos Z G 1984 *Int. J. Quantum Chem.* **25** 1003
Mazumdar S and Soos Z G 1979 *Synth. Met.* **1** 77
[13] Majumdar C K and Ghosh D K 1969 *J. Math. Phys.* **10** 1388
[14] Anderson P W 1987 *Science* **235** 1196
[15] Pauling L 1933 *J. Chem. Phys.* **1** 280
Eyring H, Walter J and Kimball G E 1944 *Quantum Chemistry* (New York: Wiley) ch. 13
[16] Rumer G 1932 *Gottingen Nachr. Tech.* 377
Tasaki H 1987 private communication
[17] Bondeson S R and Soos Z G 1980 *Phys. Rev.* B **22** 1793
[18] Chang K 1987 *Senior Thesis* Department of Physics, Princeton University
[19] Affleck I 1986 *Phys. Rev. Lett.* **56** 746; 1986 *Phys. Rev. Lett.* **56** 2763
[20] Affleck I, Gepner D, Shulz H and Ziman T 1988 unpublished
[21] Carrington A and McLachlan A D 1967 *Introduction to Magnetic Resonance* (New York: Harper and Row) p 118
[22] Affleck I 1985 *Phys. Rev. Lett.* **55** 1355